JOURNAL OF MATERIALS SCIENCE **40** (2005) 1901 – 1907

In-situ TEM observations of the coarsening of a nanolamellar structure in a cobalt based magnetic alloy

H. F. LI
School of Materials Engineering, Nanyang Technological University, Singapore, 639798

Y. L. FOO
Institute of Materials Research and Engineering, 3 Research Link S117602, Singapore

R. V. RAMANUJAN
School of Materials Engineering, Nanyang Technological University, Singapore, 639798

The thermal stability and coarsening of nanostructures is of both scientific interest and of engineering significance in order to produce thermally stable nanomaterials. Real time observations were carried out using ultra high vacuum (UHV) *in situ* TEM to investigate the coarsening process of a highly modulated nanolamellar structure obtained by crystallization of a Co based $Co_{65}Si_{15}B_{14}Fe_4Ni_2$ amorphous magnetic alloy. The coarsening process consisted of three steps: (a) precipitation of spherical fine precipitates; (b) continuous coarsening of the nanolamellar structure at the surface and precipitation at the grain boundaries; and (c) formation of a stable multiphase structure. Due to surface effects, continuous coarsening of nanolamellar structure was observed during *in-situ* annealing; this mechanism was different from that of the coarsening process found during conventional annealing. Discontinuous coarsening from grain boundaries, which dominates the coarsening process in the conventional annealing of bulk sample, also occurred in *in-situ* annealing of thin sample. The driving force for coarsening of the nanolamellar structure from interlamellar interfaces, grain boundaries and surfaces is discussed.

1. Introduction

The exploration and development of nanostructured materials is one of the focus areas of materials research [1]. Nanostructured materials are often found to have superior properties including magnetic, mechanical, thermal, electrical and chemical properties. However, the stability of these nanostructures is of great concern in several applications, since coarsening is a common phenomenon at elevated temperatures of fine microstructures [2–5]; it will result in undesirable microstructures, causing a deterioration of the properties. In conventional materials, the coarsening process can be continuous or discontinuous; it can be initiated by interfaces or by defects such as dislocations, stacking faults, grain boundaries and excess vacancies. The study of coarsening in nanostructures can predict the reliable temperature range for applications and possible pathways to stabilize the fine microstructures in order to further improve the properties. The coarsening process of nanostructures can also differ from the conventional materials [6–9], it is thus of interest in nanostructure research.

In previous work [10], a highly modulated nanolamellar structure was reported in a crystallized Co based $Co_{65}Si_{15}B_{14}Fe_4Ni_2$ amorphous magnetic alloy. This highly modulated nanolamellar structure has potential applications as nanotemplates, nanogrids, filters and catalysts. The nanolamellar structure was subsequently consumed by a heterogeneous microstructure after longer annealing time or annealing at higher temperature [10, 11]. This heterogeneous microstructure is actually the coarsened microstructure of the initial nanolamellar structure. In this paper, a real time *in-situ* TEM observation of the microstructural evolution of this nanolamellar structure is reported. A comparison of microstructural evolution between *in-situ* annealing and conventional annealing is included.

2. Experimental

This investigation started from a crystallized Co based metallic glass $Co_{65}Si_{15}B_{14}Fe_4Ni_2$ with a highly modulated nanolamellar structure (Fig. 1). The TEM sample was slightly ground to about 10 μm and then ion-milled to make it electron transparent. Real time observations were conducted in a JEM-2000V *in-situ* UHV-TEM. The sample is positioned on a 6×2 mm silicon slab, which can be resistively heated. The temperature of 500°C was obtained by controlling the current

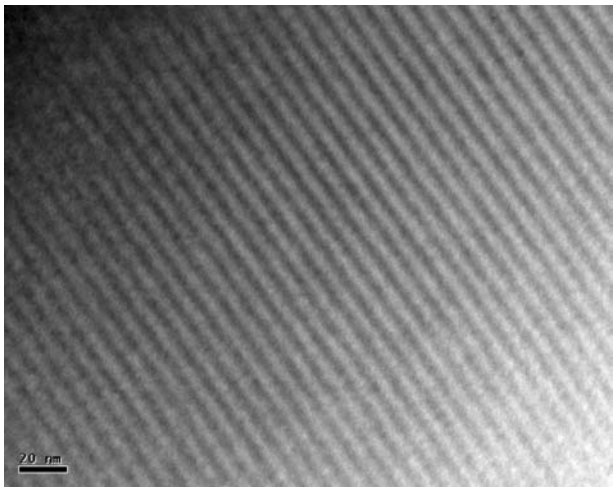

Figure 1 BF TEM micrograph of the periodic nanolamellar structure observed in the starting material.

passing through the silicon substrate (Joule heating). Conventional annealing was conducted in a vacuum furnace (10^{-5} Torr); the TEM sample was thinned using ion milling after annealing; and TEM observation used a JEOL 2010 TEM.

3. Results

The initial microstructure consisted of grains with nanolamellar structure; the nanolamellar structure was very regular with lamellar width of about 5 nm (Fig. 1). Phase transformation of this microstructure was rapid at the annealing temperature of 500°C. Fig. 2 shows the overall microstructural evolution process. From the initial highly modulated nanolamellar structure within the large grains (Fig. 2a), a high density of spherical precipitates were formed after annealing for 400 s (Fig. 2b), the nanolamellar structure underwent no change at this stage; subsequently the nanolamellar structure showed a corrugated appearance and a contrast change in some part of the grain was observed (Fig. 2c); finally, the nanolamellar structure disappeared and was transformed to a multiphase structure (Fig. 2d).

The detailed evolution process in each step is shown in Figs 3–5 respectively. The density of the spherical precipitates which appeared after just a few seconds of annealing at 500°C increased slightly after holding for longer time (Fig. 3a and b). A few precipitates grew larger while most of them did not change much in size during annealing up to 5300 s (Fig. 3c and d); at the same time, larger precipitates could be observed at the

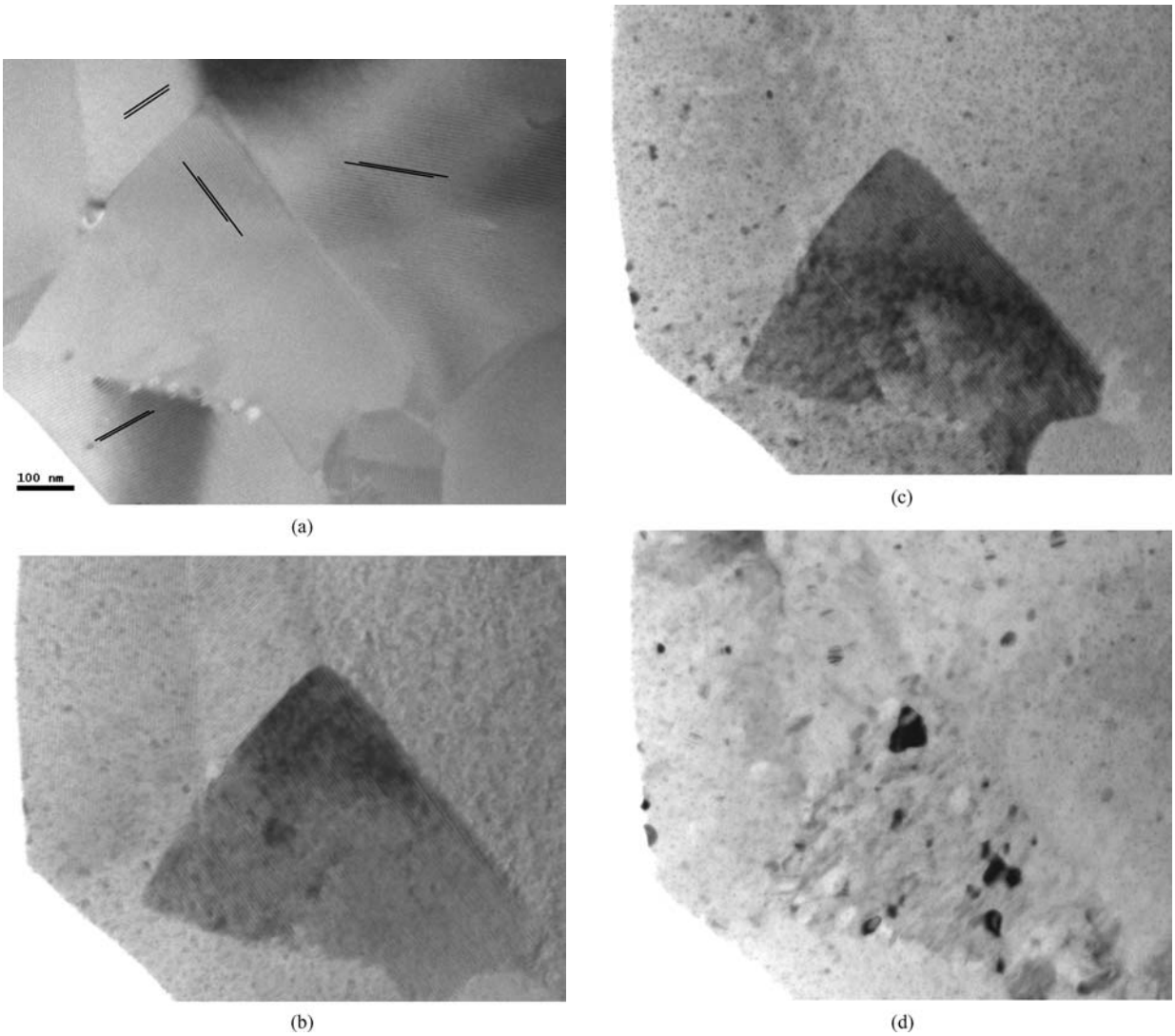

Figure 2 BF TEM micrographs, showing overall coarsening process of nanolamellar structure in a cobalt based alloy $Co_{65}Si_{15}B_{14}Fe_4Ni_2$ *in-situ* annealed at 500°C. The holding time is about (a) 0 s, (b) 400 s, (c) 2500 s, and (d) 7000 s.

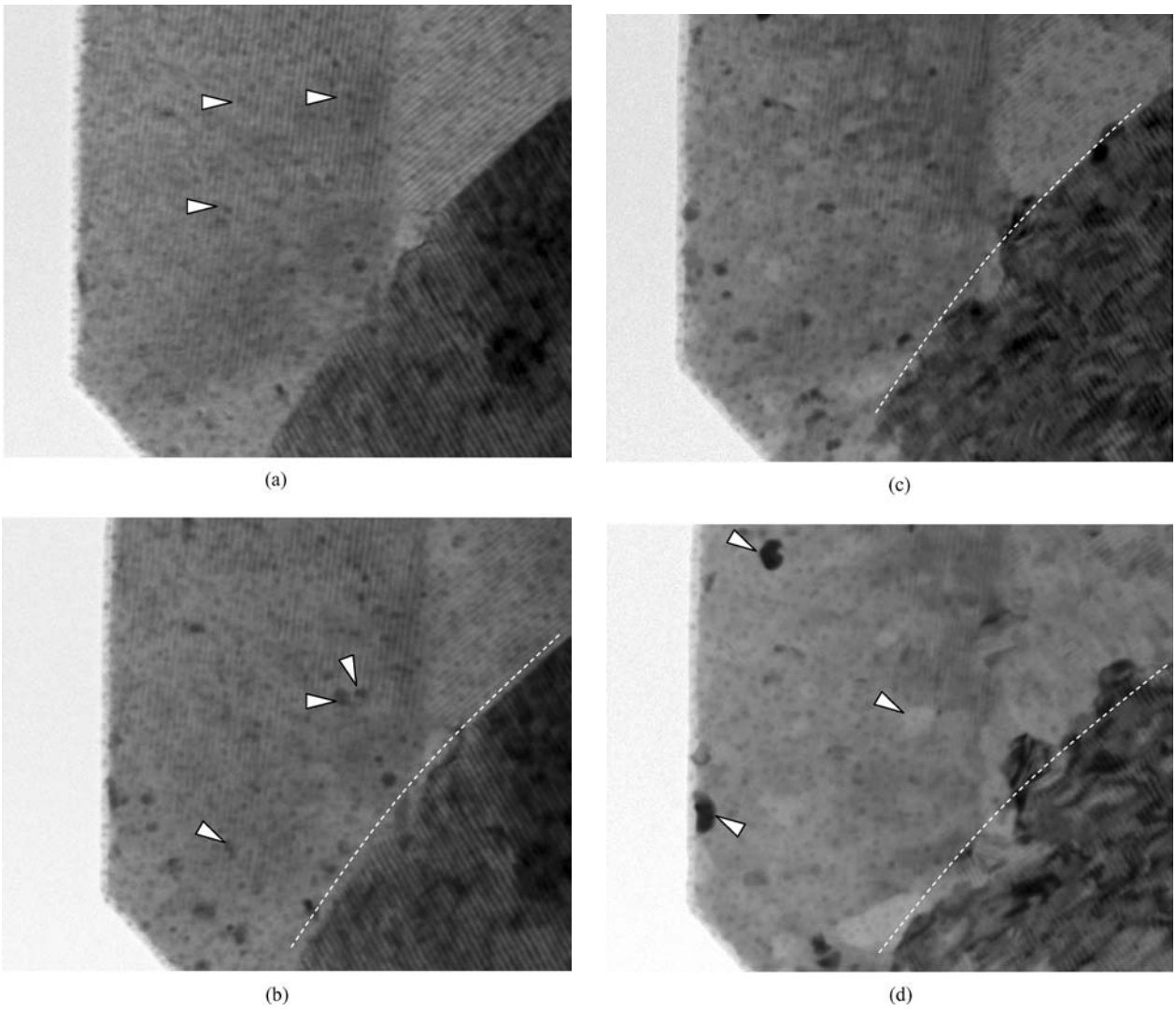

Figure 3 Spherical precipitates and evolution. *In-situ* TEM micrographs of the sample annealed at 500°C for (a) 650 s, (b) 1100 s, (c) 3700 s and (d) 5300 s. Arrows indicated the fine precipitates; the white dash line refers to the grain boundary that underwent change.

grain boundaries (dashed line in Fig. 3d). Corrugated nanolamellae were observed after holding for about 2400 s at 500°C. This distortion of nanolamellar structure became greater after holding about 3800 s (Fig. 4a); then the nanolamellar structure was consumed by a new structure which is bright in BF image (Fig. 4b); the bright area increased (Fig. 4c) and consumed the grain with the nanolamellar structure (Fig. 4d). However, the initially formed small spherical precipitates could still be observed after the disappearance of the nanolamellae. The SADPs from the grain with corrugated lamellae (Fig. 4a) and the grain after the nanolamellae was consumed (Fig. 4d) showed a difference in the intensity distribution of the reflection spots.

Further microstructural evolution was mainly initiated by precipitation at the grain boundaries (Fig. 5a and b) followed by heterogeneous or homogenous nucleation of new phases (Fig. 5c and d). The original grain with regular nanolamellar structure was finally transformed to a multiphase structure. Fig. 6 showed the coarsened nanolamellar structure from conventionally annealed samples. Fig. 6a showed the microstructure in the intermediate stage of coarsening, the nanolamellae remained the same as the initial structure while the upper part was clearly coarsened; Fig. 6b showed the final product from conventional annealing, which is a multiphase structure.

4. Discussion

4.1. *In-situ* observation of the coarsening process of nanolamellar structure

In-situ TEM (transmission electron microscopy) is a state-of-art technique, which can provide a real time observation of the microstructure evolution [12–15]. It can thus enable a better understanding of mechanisms as well as the modeling of relevant processes. From *in-situ* TEM observations, the overall coarsening process (Fig. 2) of nanolamellar structure can be described in three steps: (a) precipitation of fine precipitates, (b) change in nanolamellae, and (c) formation of a multiphase structure. The steps (a) and (c) were discontinuous coarsening process; step (b) corresponded to continuous coarsening.

In the first step, a high density of spherical nanoprecipitates was observed after annealing at about 500°C. The precipitates had a size of about 10 nm (Fig. 3a). With an increase in holding time, these precipitates did not change significantly except for a small increase in the density of the precipitates (Fig. 3b); a few

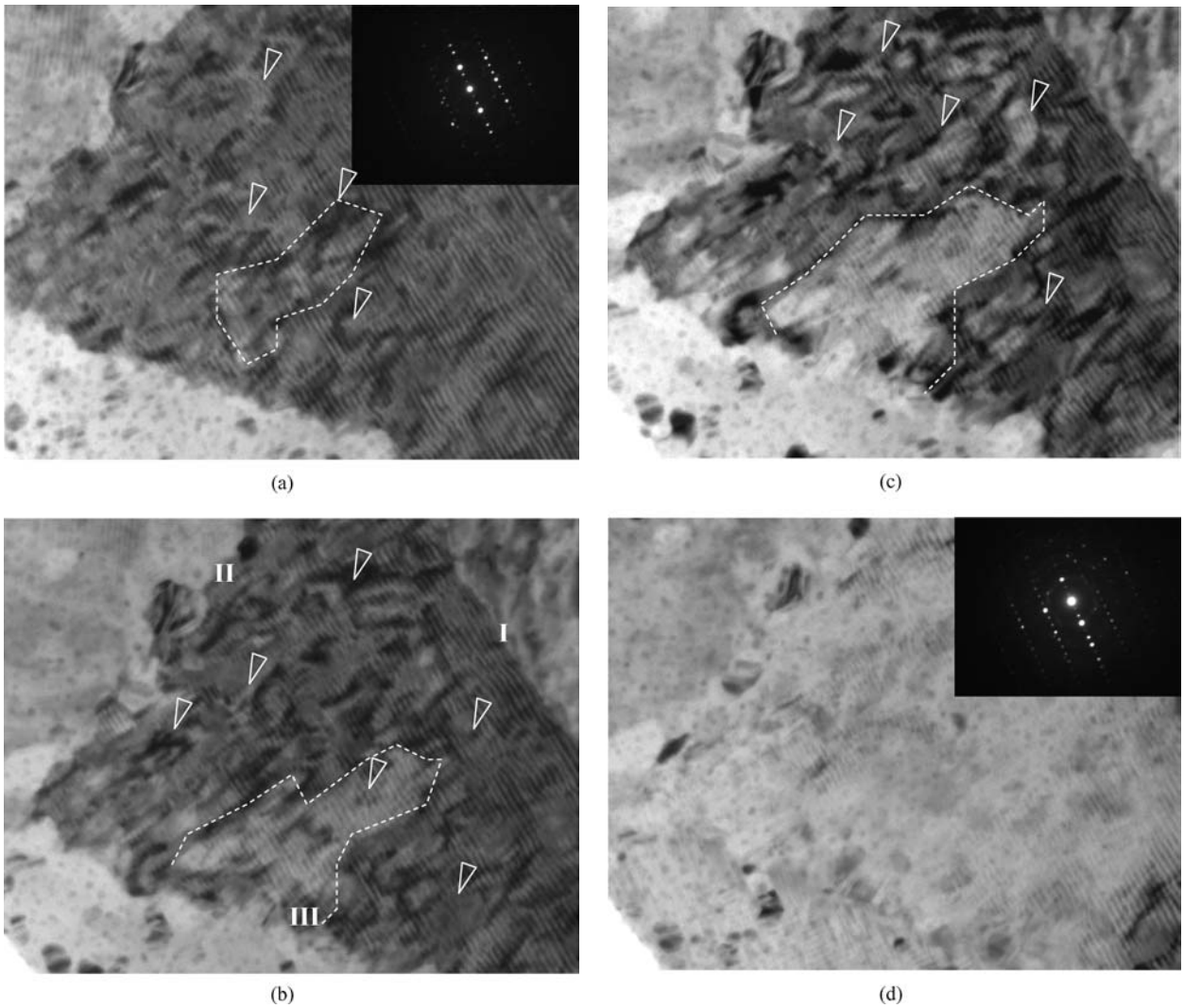

Figure 4 In situ TEM showing corrugation and disappearance of nanolamellae. (a) 3800 s, (b) 5000 s, (c) 5400 s and (d) 5900 s. The arrows refers to the corrugated regions and the bight regions. The circled bright region with dash lines increased the area with the increase in annealing time.

precipitates with larger size were observed (Fig. 3c and d). Even after very long holding time, these precipitates were observed, as in Fig. 5, when the nanolamellar structure had disappeared. From the image contrast, the precipitate appeared to have no crystallographic relationship with the nanolamellae; at the same time, no ring pattern of SADP was observed from the grains with these fine precipitates. It is therefore suggested that this precipitation is a surface effect, which could be due to surface oxidation or special atomic structures at the surface. In Byeon's work [16], oxide precipitates were formed in a crystallized substrate $Co_{74.26}Fe_{4.74}Si_{2.1}N_{18.9}$ after annealing at 250°C in air. The oxide precipitates in their work were amorphous and interpreted to be borosilicates. In our work, *in-situ* TEM was carried out in ultra high vacuum conditions, serious oxidation is not possible; however, due to trapping of oxygen atoms in the sample, release of oxygen at elevated temperature can occur and surface oxidation can take place. Although these fine precipitates did not greatly affect the nanolamellar structure, they served as a heterogeneous nucleation sites for precipitation in the third step. The large precipitates in Fig. 3d did not grow from fine spherical precipitates but were instead the discontinuously coarsened product of the nanolamellar structure.

The coarsening of nanolamellar structure actually started from a change of shape of the lamellae to corrugated morphology and discontinuous coarsening (from the grain boundaries and free surfaces). Fig. 4 shows the evolution of nanolamellae: firstly the nanolamellae became corrugated, some dark and bright areas in the corrugated region were observed (Fig. 4a); then more nanolamellae changed to a corrugated morphology and some corrugated regions appeared bright (Fig. 4b); such bright areas grew larger and finally consumed up the whole grain (Fig. 4c and d), the nanolamellar structure disappeared after this stage. The difference in SADPs from the same area with initial nanolamellar structure and when nanolamellae were consumed is related to the intensity of spots; no extra spots corresponding to the formation of new phases were observed. This indicates that the crystal structure did not change during this transformation.

Precipitation and growth of precipitates at the grain boundaries were also observed (Fig. 4). The initially straight grain boundaries were found to become zigzag due to the formation of fine precipitates at the grain boundaries (Fig. 4a); these fluctuations in the grain

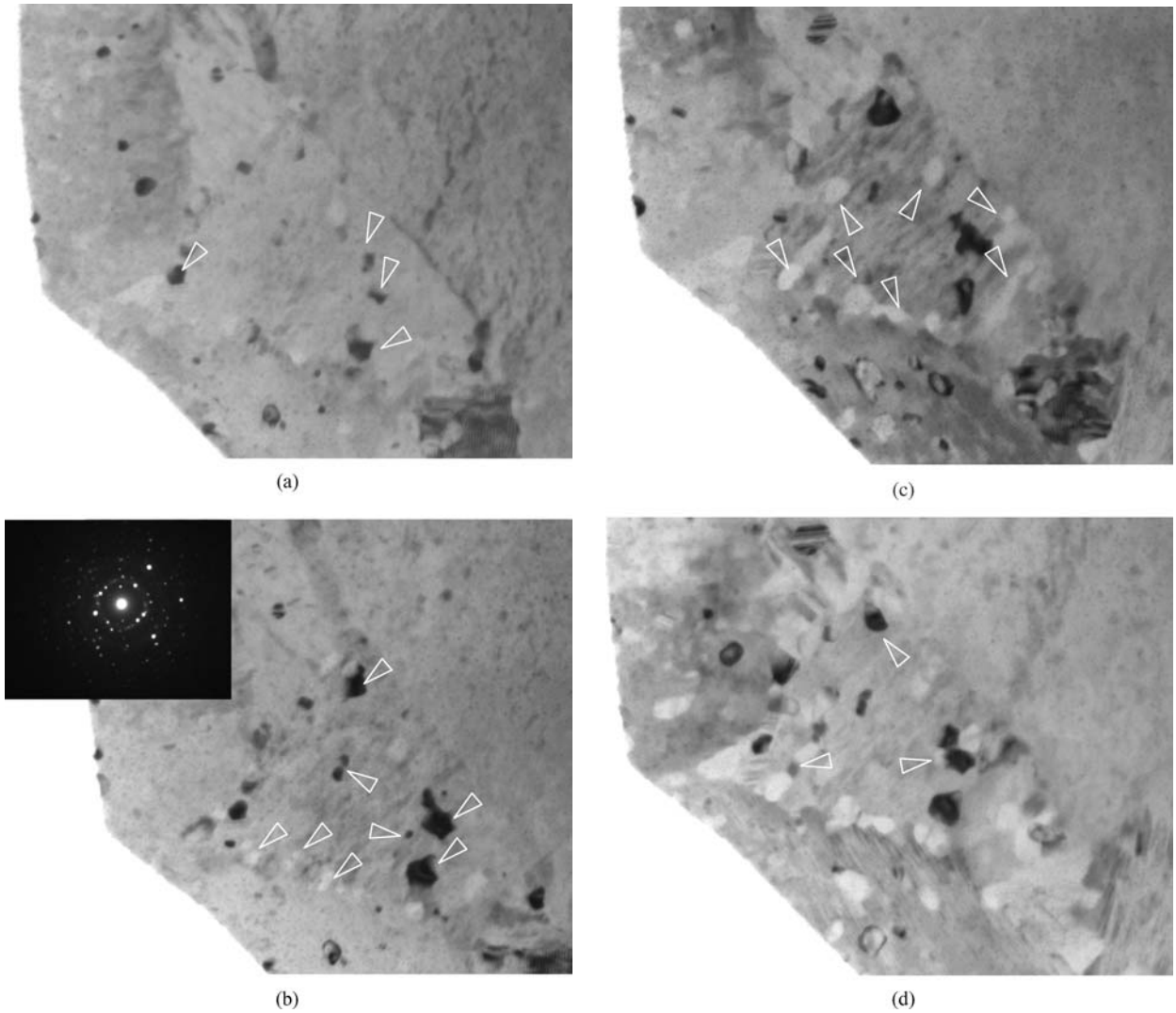

Figure 5 Further transformation after disappearance of nanolamellar structure. (a) 6350 s, (b) 6550 s, (c) 7800 s and (d) 8150 s. The arrows in (a) and (b) refers to the black precipitates. The arrows in (c) and (d) indicated the white precipitates and heterogeneously formed precipitates.

boundary became larger with increasing holding time (Fig. 4b and c). This is a discontinuous coarsening process of the nanolamellar structure. It can also be seen that this type of coarsening depends on the orientation relationship of the nanolamellae with the boundary and lamellae in neighboring grains [17]. As indicated in Fig. 4b, very little change in grain boundary I occurred although in boundary II and III large changes had taken place. Boundary I is nearly parallel to the lamellae while boundary II and III have a high angle with the boundary as well as the neighboring lamellae in boundary II and III. This difference can be attributed to the atomic segregation to the boundary and their geometry of the interface, as discussed later.

The third step is a multi-phase formation process. As the equilibrium phases from Co-Si-B ternary phase diagram [18] are Co_2Si, Co_2B and h.c.p. Co for a composition close to the alloy composition used in this investigation, transformation into these phases is enabled when the diffusion of atoms is high enough. The mobility of atoms in the surface and defects such as dislocations, stacking faults and grain boundaries is usually higher. Therefore, this step started from the surface by heterogeneous nucleation at the fine spherical precipitates formed in the first step as well as from the grain boundaries. As shown in Fig. 5, large precipitates (black in contrast) were observed (Fig. 5a); subsequently most of them increased in size and some new precipitates were observed (white in contrast) near the grain boundaries (Fig. 5b); these new precipitates became larger and more precipitates (bright in contrast) could be seen while some of the initial precipitates (dark in contrast) decreased in size or disappeared, these new precipitates were mainly located near the grain boundaries or close to the initial precipitates (black in contrast) (Fig. 5c); finally the multiphase structure was formed (Fig. 5d). A similar precipitation process was also observed in other grains. From the microstructural evolution in this third step, it can be concluded that the precipitate formed earlier is metastable; the precipitates formed later caused the dissolution of these earlier formed precipitates, they also consumed some of the matrix phase; equilibrium composition was then reached and a mixture of phases formed. From earlier report, it is expected that these two types of precipitates were Co_2Si and Co_2B phases. In Fig. 5c and d, some faulted precipitates were observed, which correspond to the Co phase.

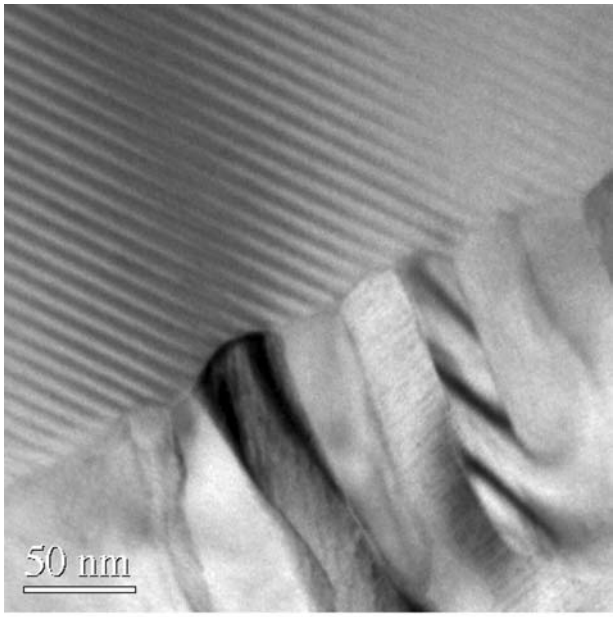

(a)

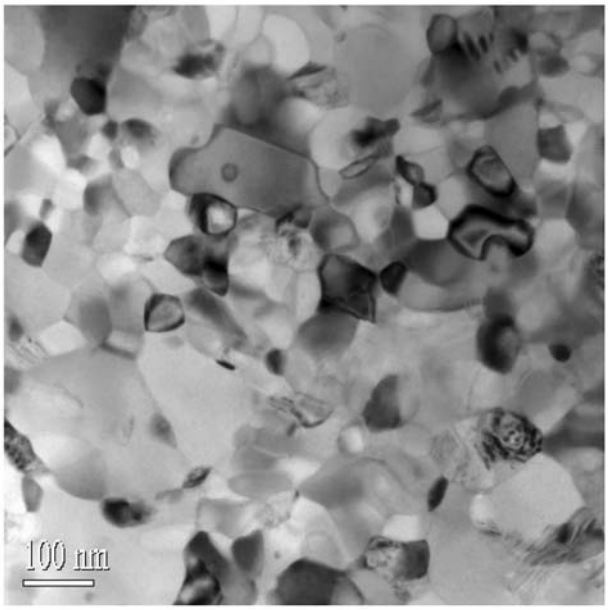

(b)

Figure 6 Conventional coarsening process. (a) 530°C for 60 min and (b) 600°C for 60 min.

The time periods for these three steps are not separated but overlap. For example, discontinuous coarsening from grain boundaries actually involved the formation of multiphase mixtures which should belong to the third step; however it occurred almost at the same time as nanolamellae corrugation in the second step. Comparison of these processes can provide information on the effect of grain boundaries, lamellar interfaces and the surfaces on the coarsening of nanolamellae. This will be discussed in detail in Section 3 of discussion.

4.2. Comparison of *in-situ* coarsening and conventional coarsening

The difference in the coarsening process of *in-situ* and conventional annealing is due to surface effects. In *in-situ* annealing, a thin foil sample was used, in which a large portion atoms are at or near the surface, the surface effects thus play a significant role in coarsening.

Fig. 6a shows the conventionally annealed sample, it can be observed the nanolamellar structure retains good periodicity although a large portion of the lamellar structure was consumed by the discontinuous coarsened microstructure. This discontinuous coarsening was initiated by the grain boundary. This is different from the *in-situ* coarsening process in which the nanolamellar structure was corrugated together with the discontinuous coarsening from the boundaries (Fig. 4). Fig. 6b showed the final microstructure from conventional annealing, which consisted of similar near-spherical grains to the final product of *in-situ* annealing. In our previous paper [11], the phases were tentatively interpreted to be a mixture of Co_2Si, Co_2B, h.c.p. & f.c.c. Co and Co_4B.

It can thus be concluded that surface effects have a significant effect on the process of the coarsening while it has less effect on the final product. The surface effect led to a continuous coarsening of the nanolamellar structure and formation of a metastable phase which has a crystal structure similar to that of the original nanolamellae. The discontinuous coarsening from the grain boundaries was also affected by surface effects. In conventional annealing, discontinuous coarsening led to a coarse lamellar structure which consisted of several phases, due to the large interfacial energy between the lamellae they were metastable and broke up into near spherical grains. In the case of the *in-situ* annealing, discontinuous coarsening started by the nucleation of one phase at the grain boundaries; then heterogeneous nucleation of another phase from the first phase occurred and a multiphase microstructure was thus formed.

4.3. Thermodynamic explanation of the coarsening process

Microstructures try to reach a minimum energy but are kinetically controlled by the diffusion [19], the coarsening process occured mainly due to the large interfacial energies. The instability of the nanolamellar structure in this investigation can be attributed to the energy of the metastable crystal structure, composition of the lamellar structure and the interfacial energy between the nanolamellae.

To determine which coarsening process will dominate, one needs to consider the driving force of continuous and discontinuous coarsening. For the nanolamellar structure, a coherent interface is assumed, the interfacial energy of nanolamellae is mainly due to change in the bonding environment of the atoms at the interface (Fig. 7). $\gamma_{\text{ch-A}}$ is used to represent this type of interfacial energy. At the grain boundaries, the interfacial energy will include contributions due to the change in bonding of atoms at two neighboring grains $\gamma_{\text{ch-B}}$, the strain energy $\gamma_{\text{ch-C}}$ and also the interfacial energy of nanolamellae $\gamma_{\text{ch-A}}$. At the surface, the energy making the structure unstable includes contributions from atoms in the surface layer $\gamma_{\text{ch-D}}$ and $\gamma_{\text{ch-A}}$. The driving force per unit area for the coarsening of a small volume selected from interlamellae, different grain boundaries and surface (as schematically illustrated in Fig. 7) can

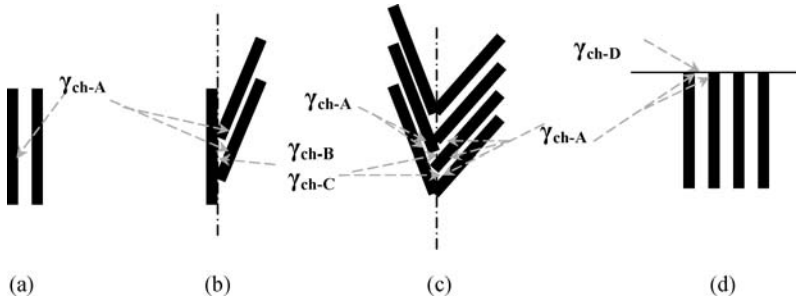

Figure 7 Schematic interfacial conditions with nanolamellar structure. (a) Interlamellae, (b) grain boundary oriented parallel to the nanolamellae of one neighboring grain (Grain boundary I), (c) grain boundary having a large angle to the nanolamellae, (d) free surface with nanolamellae perpendicular to the surface.

be represented as

(a) Interlamellae. $F_I = \gamma_{ch\text{-}A}$

(b) Boundary I. $F_{B\text{-}I} = 2\gamma_{ch\text{-}A} + 2\gamma_{ch-B} + 2\gamma_{ch\text{-}C}$

(c) Boundary II $F_{B\text{-}II} = (>4)\ \gamma_{ch\text{-}A} + (>2)\ \gamma_{ch-B} + (>2)\ \gamma_{ch\text{-}C}$

(d) Surface $F_S = 2\gamma_{ch\text{-}A} + \gamma_{ch\text{-}D}$

The number used before the γ in the above equations represents how many such interfaces involved (as indicated in Fig. 7). From this estimate, it is obvious that boundary II has the highest energy and the energy of interlamellae is smallest. The driving force at the surface may be large since atoms with unsatisfied bonds can have much higher interfacial energy. Therefore continuous coarsening occurring directly at the interlamellar interface is difficult compared to the coarsening from the boundaries and surfaces. Grain boundaries can act as nucleation sites of the stable phases, thus discontinuous coarsening can easily occur from the grain boundary II.

At the surface, due to capillary effects, a straight surface with perpendicular nanolamellar interface (or other non-parallel configurations) was found to be unstable, thus the interface will become wavy. In order to further reduce the energy, the wavelength will increase, thus continuous coarsening from the surface can occur.

5. Conclusions

A real time *in situ* hot stage TEM investigation of the coarsening process of the nanolamellar structure was carried out.

(1) From the observations the coarsening process can be described in three steps: (a) precipitation of spherical fine precipitates; (b) continuous coarsening of the nanolamellar structure from the surface and precipitation at the grain boundaries; and (c) formation of a stable multi-phase structure.

(2) Surface effects play a significant effect in the coarsening of nanolamellar structure in the thin foil, leading to different coarsening processes in *in-situ* compared to conventional annealed samples. Considerable continuous coarsening was observed in the *in situ* annealed sample, while this was virtually absent in the conventionally annealed samples.

(3) The final products of coarsening by *in-situ* and conventional annealing are similar.

(4) Discontinuous coarsening from the grain boundaries dominated the coarsening of nanolamellar structure. The orientation relationship of grain boundaries with the nanolamellae and the orientation relationship of nanolamellae in the neighboring grains also affected the coarsening process.

References

1. H. GLEITER, *Acta Mater.* **48** (2000) 1.
2. J. W. MARTIN, R. D. DOHERTY and B. CANTOR, "Stability of Microstructure in Metallic Systems", 2nd ed. (Cambridge University Press, 1997) p. 219.
3. J. C. ZHAO and M. R. NOTIS, *Acta Mater.* **46** (1998) 4203.
4. G. SHARMA, R. V. RAMANUJAN and G. P. TIWARI, *ibid.* **48** (2000) 875.
5. S. VEPREK and M. JILEK, *Vacuum* **67** (2002) 443.
6. A. L. GREER, in Proc. 22nd Risø Inter. Symp. Mater. Sci.: Science of Metastable and Nanocrystalline Alloys, Structure, Properties and Modeling, edited by A. R. Dinesen, M. Eldrup, D. Juul Jensen, S. Linderoth, T. B. Pedersen and N. H. Pryds, A. Schrøder Pedersen and J. A. Wert, (Denmark, 2001) p. 461.
7. J. LEE, F. ZHOU and K. H. CHUNG, *Metall. Mater. Trans.* A **32** (2001) 3109.
8. F. LIU and R. KIRCHHEIM, *J. Cryst. Growth* **264** (2004) 385.
9. H. TANIMOTO, P. FARBER, R. WÜRSCHUM, R. Z. VALIEV and H. E. SCHAEFER, *Nanostruct. Mater.* **12** (1999) 681.
10. H. F. LI and R. V. RAMANUJAN, *Intermetallics* **12** (2004) 803.
11. *Idem.*, *Mater. Sci. Eng.* A **375–377** (2004) 1087.
12. N. NISHIYAMA, M. MATSUSHITA and A. INOUE, *Scripta Mater.* **44** (2001) 1261.
13. L. TAN and W. C. CRONE, *ibid.* **50** (2004) 819.
14. S. X. ZHOU, Y. G. WANG, J. H. ULVENSØEN and R. HØIER, *IEEE Trans. Magn.* **30** (1994) 4815.
15. F. ZHOU, K. Y. HE and K. LU, *Nanostruct. Mater.* **9** (1997) 387.
16. S. C. BYEON, C. K. KIM, K. S. HONG and R. C. O'HANDLEY, *Mater. Sci. Eng.* B **56** (1999) 58.
17. R. V. RAMANUJAN, P. J. MAZIASZ and C. T. LIU, *Acta Mater.* **44** (1996) 2611.
18. P. VILLARS, A. PRINCE and H. OKAMOTO, "Handbook of Ternary Alloy Phase Diagrams" (computer file) (ASM international, Materials Park, 1997).
19. D. A. PORTER and K. E. EASTERLING, "Phase Transformations in Metals and Alloys", 2nd ed. (Chapman & Hall, 1992).

Received 7 October
and accepted 10 December 2004